

---



---

## EXPERIENCES WITH TESTING PCRV CONCRETE AND EPOXY RESIN MODELS

K. SCHIMMELPFENNIG, G. SCHNELLENBACH  
Zerna-Schnellenbach, Consulting Engineers,  
Bochum,  
Federal Republic of Germany

### 1. Introduction

Within the scope of the PCRV research program sponsored by the German "Minister für Forschung und Technologie" and other activities concerning PCRVs, several model tests have been carried out at the Ruhr-Universität Bochum during the years past.

Object of one test series was to investigate the operating behaviour of a PCRV, which is only partially prestressed. For tests like these a large concrete model is necessary. The authors had the opportunity to use the 1:5 scale model of the PCRV of Schmehausen THTR nuclear power plant for this purpose.

Further experimental work was done in manufacturing and testing epoxy resin models in order to improve the results of three-dimensional numerical calculations.

This report gives a survey on the work carried out and the results gained.

### 2. Testing a large scale concrete model

#### 2.1 Purpose of the test program

Prestressed concrete reactor vessels built in Europe up to now had to be designed under the condition that tensile stresses



Fig. 25. Half-thickness model after testing.

are strictly limited in undisturbed regions of the vessel walls. For a vessel designed like that, cracking, thus, can be excluded except in local regions. But the consequences are vessel designs with large wall dimensions and very strong prestressing, that means: high costs. Hence, it becomes desirable to attain a more economic vessel design by using the concept of so-called partial prestressing, which allows cracking to a great extent even under operating conditions.

Hitherto, no experience of operating behaviour of such partially prestressed concrete reactor vessels has been gained. A good chance for closing this leak of knowledge was given by the fact that in 1972 the mentioned 1:5 scale model of the THTR vessel was still ready for further use, after the tests in order to confirm the design concept of this vessel had been finished. The authors and several other members of a research group at Bochum University, managed by Prof. Zerna and the co-author, made use of this opportunity and carried out tests with this model in order to investigate behaviour under partial prestressing.

The previous tests had been short-time and long-time cycles with internal temperatures and pressures corresponding to normal operating conditions of the prototype, and subsequently cycles with stepwise increasing pressure up to 2.1 times the operating pressure, that is 85 bar. These overload tests, which yielded cracking (as shown later on), had been demanded for ultimate load analysis, in order to conclude from crack development and deformation measurements on formation of a kinematic failure mechanism.

These cracks having occurred at loads significantly above operating pressure of 40 bar, were considered to exist already under service conditions in the following tests. Thus, 61 bar internal pressure was chosen as - say - new operating pressure. Simultaneously, the influence of higher temperatures than those,

imposed on concrete vessels until now, on service behaviour had to be investigated. The aim was to show that higher temperature gradients can be allowed for partially prestressed vessels without any disadvantage in operating behaviour and safety. Besides saving costs due to reduction of wall thickness and prestressing, this would lead to a more economic design of insulation and liner cooling system.

The general purpose of the test programm was to demonstrate that a partially prestressed vessel under arbitrary load histories behaves at least as well as a conventional fully prestressed vessel. So, hot and cold phases as well as long-time and short-time pressure cycles were provided submitting the vessel to heavier load conditions than usual today (see /1/, /2/).

## 2.2 Description of model and test procedure

The model geometry is shown in Fig. 1. In general the prototype has been scaled down. Only relative thicknesses of liners have been enlarged, and numbers of prestressing tendons have been reduced, the prestressing degree however being identical to the prototype.

In order to grant a uniform and constant temperature distribution in the water used as hydraulic liquid during the periods with 80 °C internal temperature, a special agitating device for circulating the water was constructed and fixed in one of the steam-generator penetrations. Originally, more than 700 measuring transducers were installed. Here, only those types shall be mentioned the results of which are discussed in the following. Local strains of concrete were measured by concrete strain transducers (BDG), based on strain gauge technique; they were installed in one, two or three directions in the measuring points. Since these can only be used for short-time measurements, vi-

brating wire transducers (SDG), which are long-time stable, were arranged additionally. Furthermore, inductive displacement transducers (DFG) were installed on a separate frame in order to measure displacements of the outer surfaces and along certain lines on the surface in order to investigate the behaviour of cracked regions.

The test procedure during the research program on partial prestressing is outlined in Fig. 2. Firstly, a temperature gradient of 40 °C was attained in the walls by heating the cavity water to 80 °C and controlling the environment by an air conditioning equipment. After an unpressurized period (called period 14), some short-time pressure cycles with 30, 40 and 50 bar pressure above atmospheric were carried out. Here and in the following figures the dimension "bar" means a pressure above atmospheric.) After another seven weeks hot-unpressurized state, two short-time 60 bar cycles were run, and subsequently seven weeks pressure, called period 16. A second long-term pressure period of four weeks was carried out after three weeks of interruption. Then temperature was lowered stepwise with interruptions of one week, short-time 60 bar pressure cycles being undertaken during this period. By this load history - with regard to the former tests carried out with this model - operating conditions were simulated, which are surely more serious than those being applied to a reactor vessel under very pessimistic assumptions. A satisfactory behaviour of the model under these conditions would demonstrate the suitability of the partial prestressing concept.

### 2.3 Model behaviour under short-time pressure cycles

Response of the vessel model on short-time pressure cycles shall be outlined by discussing results from a few characteristic measuring points. The chosen concrete strain transducers are situated on three lines, as shown in Fig. 3. In all these regions cracking has already occurred during former test periods, at the

outer surface at line V near the center of the bottom slab and at line XI between blower penetrations, and on the inner surface around line XIII, running inclined upward from the upper slab-wall junction.

In all these regions, influences of the elevated temperature gradient can be recognized, but the effects due to cracks at the outer surface are different from those at the inner surface. In Figures 4 and 6, strains in dependence of internal pressure under two different temperature gradients are plotted for lines V and XI with cracking at the outer surface. Due to temperature loading, the outside is already pre-strained. Thus, higher temperatures yield deeper propagating of the neutral plane into the wall than lower temperatures, if internal pressure is applied additionally. This leads to a uniform elevation of the strain level of the pressurized vessel with increasing temperature gradient. Over the whole time of testing, strain plots corresponding to 60 bar pressure, as shown in Figures 5 and 7 for the same measuring lines, consequently indicate decreasing strains due to internal pressure, when temperature decreases during the final test period. Since in the meantime cracking has propagated - particularly during the hot-pressurized periods - modifying the mechanical system of the vessel, strains do not fully remove towards the values measured formerly under the same pressure and temperature conditions.

At the slab-wall junction (line XIII), the situation is different from those mentioned before (Figures 8 and 9). Cracks existing from previous over-pressure tests, are closed and compressed due to temperature loads, if the vessel is unpressurized. Compression stresses concentrated in this region are significantly redistributed due to creep, particularly under elevated temperatures. In consequence - although conditions are different from those mentioned before - also here tensile strains under internal pressure following a period under 80 °C tempe-

ature without pressure, are higher than under 40 °C. Decreasing strains of transducer 298 at the inside during decreasing temperature in the final test period indicate that the whole structure becomes stiffer again due to closing of cracks, leading to decreasing displacements between cylinder and top slab under internal pressure.

#### 2.4 Model behaviour under long-time pressure

During the first period under 60 bar long-time pressure combined with 80 °C internal temperature, cracking propagated considerably. In Fig. 10 typical crack patterns on the vessel surface are shown, left-hand the state after the first overpressure test, right-hand the recent state. Particularly between the blower-penetrations a lot of fine horizontal cracks have occurred with spacings from 10 to 25 cm.

A crack pattern like this is typical and expected for a partially prestressed concrete vessel. Cracks are well distributed, crack widths, thus, being small enough. The maximum value measured has been 0.13 mm.

Overall deformation behaviour of the model during long time pressure periods has been measured by displacement transducers placed on frames around the vessel surface. Displacements thus measured are shown in Figures 11 and 12 for different times during the two long-time pressure periods. Deformations remain nearly unchanged during the single periods and also for both periods in comparison. Thus, it can be concluded that the deformations are fully reversible, even after long periods of service.

#### 2.5 Creep during the whole time of testing

Creep of the model can be discussed by using values gained from vibrating wire transducers, since these are long-time stable.

In Figures 13 and 14, strain versus time are plotted for two different groups of transducer positions. In Fig. 13, circumferential strains at the vessel equator are shown, in Fig. 14, vertical strains near the upper and lower slab-wall junctions are outlined.

In the heating phase (number 13) measurements are governed by concrete strains due to non-uniform temperature rise and temperature sensibility of the transducers. Changes of strain during this time, thus, are to a minor extent influenced by creep. Afterwards, strains in midheight of the vessel decrease continuously as long as the model is hot and unpressurized. This is mainly caused by creep due to elevated temperatures. Maximum radial displacement of the wall during this period is about -0,2 mm. When internal pressure is acting hardly any displacement occurs, since the circumferential direction is nearly unloaded and consequently there is no creep. During the final unheating period, changes of strain arising in the heating phase are removed, creep strains remaining only. The transducers measuring vertically near the inner corners (Fig. 14) do not show any change of strain during the hot unpressurized period. Here, creep of concrete yields stress redistributions due to deformation restraint - as mentioned before. Hence, no alterations of strain can be indicated. Oscillations during periods with internal pressure - particularly at the inner measuring points in the vicinity of cracks - are resulting from the greater sensibility of cracked regions and from the fact, that the plotted strains, which are related to zero-pressure, are recalculated from strains measured under 60 bar pressure in these periods. Also here, changes of strain during heating are removed in the final unheating phase. (Transducer 55 has been obviously damaged.)

These and further experimental data demonstrate that no surprising long-time effects arise with a partially prestressed concrete vessel even under temperatures up to 80 °C. Each of the test results might be analysed by the existing computing methods.

## 2.6 Conclusions

The results gained from testing the THTR 1:5 scale model under elevated pressures and temperatures, a small part of which has been shown here, allow the conclusion that under these loading conditions a partially prestressed vessel will operate reliably. Deformations under internal pressure - short-term as well as long-term - are essentially reversible. Once the final crack pattern is obtained, also varying temperatures can be applied without any significant influence on further behaviour. Influence of creep under elevated temperatures is as expected.

Computing methods existing today allow a good simulation of cracking and creep effects. Since safety of a vessel like that is not differing from that of vessel usual today, and since economic advantages can be expected, partial prestressing should be taken into consideration in future PCRV design.

## 3. Testing epoxy resin models

### 3.1 Purpose of the tests

The purpose of small scale epoxy resin models is obviously different from that of large scale concrete models. Analogy to a prototype is restricted to the geometry, since prestressing, reinforcement, liner and concrete with its special characteristics are not simulated. The material used behaves elastically and has elastic coefficients different from those of concrete in its elastic domain. Elastic behaviour without significant time dependent influences, however, makes epoxy resin a suitable material for measuring elastic strains in order to compare them with calculated values. Thus, the purpose of epoxy resin models is checking the validity of computer calculations. Modelling the geometries of PCRVs allows additionally improving the suitability of a computer program for this special geometry.

A further aim of the tests described in the following was testing a new technique of embedding strain gauges inside the model walls instead of applying them on the outer and inner surfaces only. For the further information about these tests see /3/, /4/.

### 3.2 Model manufacturing

Manufacturing of thick-walled epoxy resin models implies a lot of special problems to be solved, particularly if strain gauges have to be embedded inside the walls. There are special demands on homogeneity, accuracy of dimensions and material characteristics. Thus, an appropriate kind of resin, a suitable type of strain gauge and glue for fixing the gauges have to be chosen, a special mould and fixing technique for embedded strain gauges have to be developed.

For the models described here a warm-hardening epoxy resin, foil strain gauges and a cold-hardening resin combination for fixing the transducers have been chosen. Both resin materials have nearly identical characteristics. The models were cast in two halves with a joint at the equator. During the casting and hardening procedure, the exothermal reaction of the resin material in combination with its low thermal conductivity had to be carefully observed. Hence, an air cooling system has been arranged in the inner mould, see Fig. 15. Shrinkage of the resin due to the chemical reaction and the cooling down had to be regarded, too. In order to avoid cracks in the model due to these phenomena, the surface of the inner mould was made from Silicon caoutchouc cast on a layer of "Styropor", which was fixed on a steel tube as basic mould. Fig. 16 shows such an inner mould.

In this figure, the supports for the embedded strain gauges can also be seen. The kind of mould chosen allowed a safe adjustment of these supports. In Fig. 17, one of them is shown in detail with the strain gauges at the upper side and the wiring and connections in the middle and downside.

As outside mould a steel tube has been used, which gave no problems with heat transfer. It can be seen in figure 18, which also shows the whole mould ready for casting with steel beams for supporting and adjusting the inner mould.

After casting and hardening, the model halves were carefully measured and turned to size. Then, both halves were glued together by cold hardening resin. In Fig. 19, the THTR model can be seen ready for testing. Fig. 20 shows a detail of the upper region.

The second model had the geometry of the Hartlepool vessel, as already mentioned (see Fig. 21). The inner mould with the cores for the central cavity and the 6 steam generator cavities is shown in Fig. 22, Fig. 23 shows the upper half of the model after removing the mould, and the completed model can be seen in Fig. 24.

### 3.3 Test results

For comparison with the THTR model results, both an axisymmetric and a three-dimensional calculation has been carried out. In Fig. 25, vertical displacements of the outer surface of the top slab are shown. In the section between the steam generator penetrations, the values of the axisymmetric calculation, too, are in good agreement with the other ones. Circumferential stresses at the same surface are plotted in Fig. 26. Due to the influence of the penetrations, there is a difference between axisymmetric calculation results and measured or three-dimensionally calculated results. The agreement between the latter ones, however, is good. The same quality of results has been obtained at the outside of the cylindrical walls. Fig. 27 shows a comparison of circumferential stresses at this surface. The influence of the blower penetrations on the state of stress can be very well recognized. Finally, results from measuring points inside the walls in the haunch region are plotted in comparison with results of the axisymmetric calculation, see Fig. 28. The fi-

gure shows stresses along two lines around the haunch and a horizontal line in the cylinder wall with directions parallel to these lines.

For comparison with the Hartlepool model results, no calculations have been carried out until now due to lack of time and money. Nevertheless, some of the test results shall be shown in the following.

The first figure (Fig. 29) shows circumferential stresses at the outer surface of barrel and top cap. Deviation from axisymmetry due to the pods can be well recognized. At the inner surface (Fig. 30), circumferential stresses in the equator region are nearly undisturbed, whereas in the haunch region stress peaks due to the horizontal penetration are existing. Concentration of circumferential stresses around a pod in the equator plane is demonstrated in Fig. 31, and the last figure (Fig. 32) shows principal stresses in the haunch region in a plane between penetrations. Particularly this plot demonstrates the good success of the strain gauge embedding technique.

### 3.4 Conclusions

The above presentations about epoxy resin models have shown that manufacturing of such models - also with complicated geometries and embedded strain gauges - can be carried out fully satisfying, and that the results gained are a good tool for checking computer calculation methods.

### References

- /1/ STÖVER, R., "Versuche am 1:5-Modell des THTR-Spannbetonbehälters zur Untersuchung des Verhaltens bei partieller Vorspannung", Deutscher Ausschuss für Stahlbeton, Spannbeton-Reaktordruckbehälter-Tagung, Berlin, 13. und 14. Oktober 1975.
- /2/ SCHIMMELPFENNIG, K., SCHNELLENBACH, G., "New experiences with partial prestressing of PCRV based on large model tests", 4th Int. Conference on Structural Mechanics in Reactor Technology, San Francisco (1977).
- /3/ STÖVER, R., "Modelluntersuchungen für Spannbeton-Reaktordruckbehälter", Konstruktiver Ingenieurbau - Berichte, Vulkan-Verlag, Essen, 23 (1975) 60.
- /4/ STÖVER, R., Experimentelle Bestimmung des räumlichen Spannungszustandes eines Reaktordruckbehältermodells, Schriftenreihe des Deutschen Ausschusses für Stahlbeton, Verlag W. Ernst & Sohn, 262 (1976).

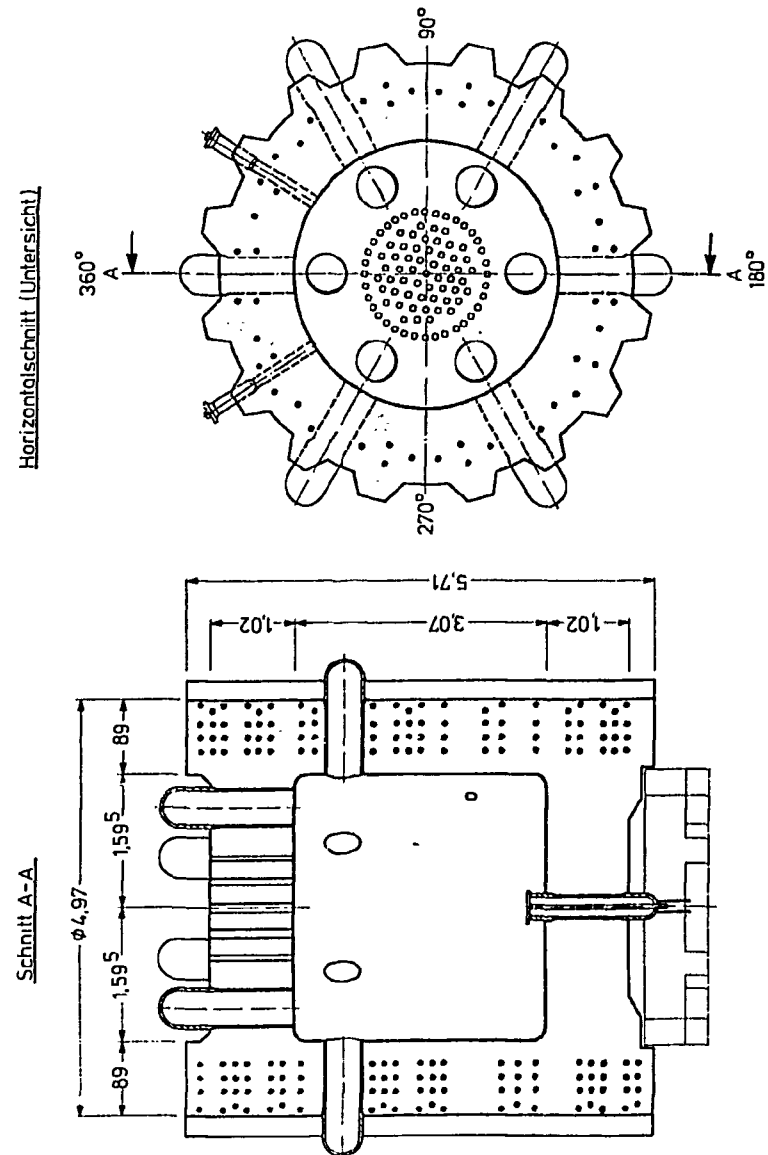


Fig. 1  
Geometry of the THTR 1:5 scale model

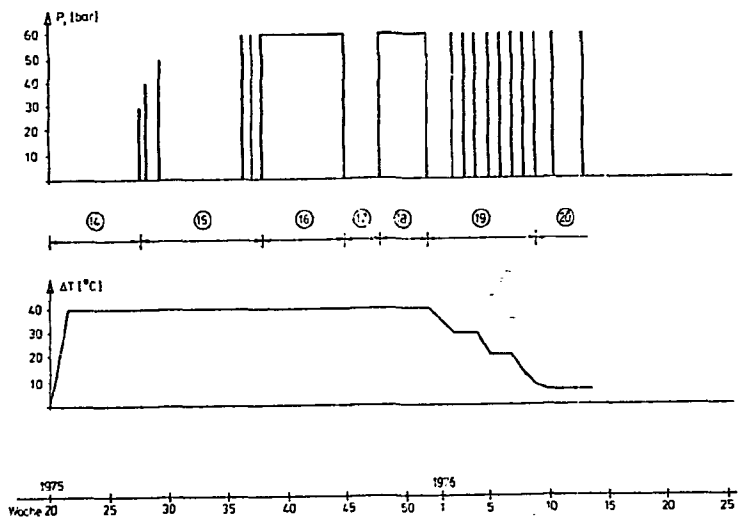


Fig. 2  
Test programm for THTR model

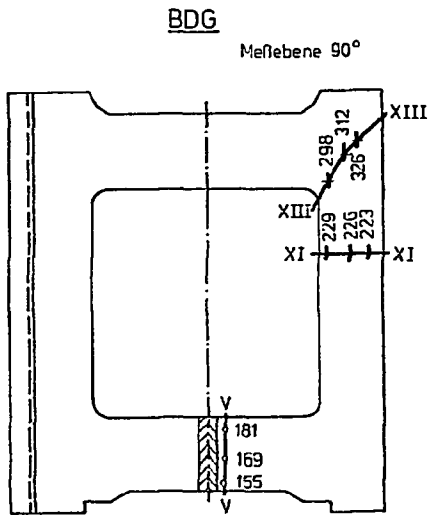


Fig. 3  
Transducer positions  
for test results in  
Figures 4 to 9

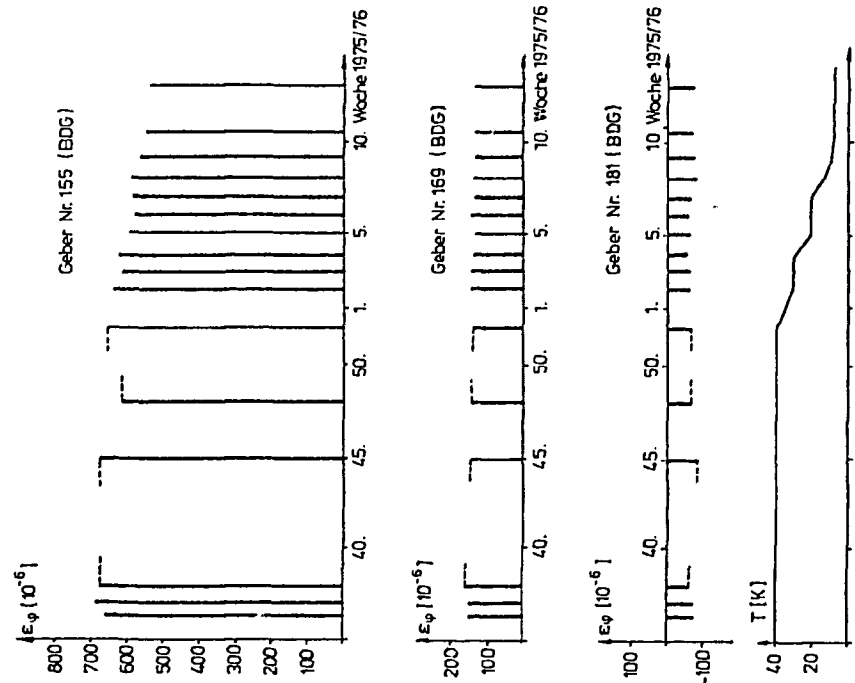


Fig. 5 Strains under 60 bar pressure, line V

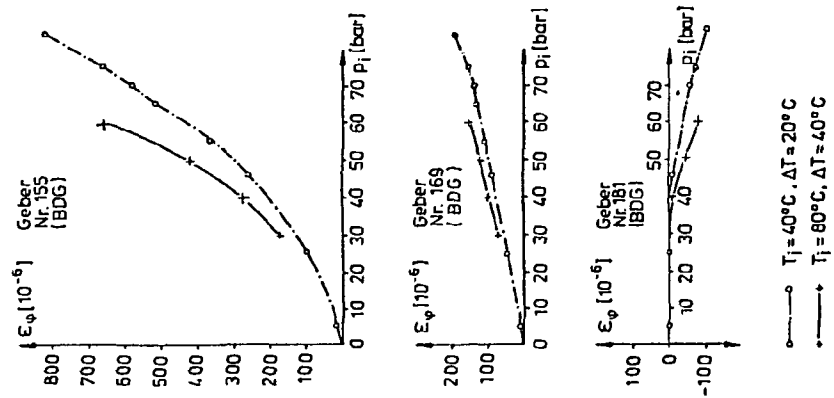


Fig. 4  
Strains versus load, line V



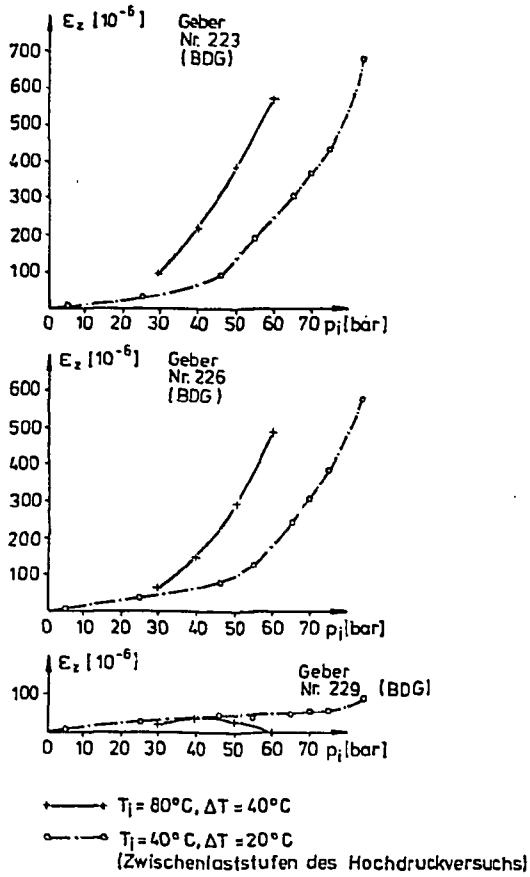


Fig. 6 Strains versus load, line XI

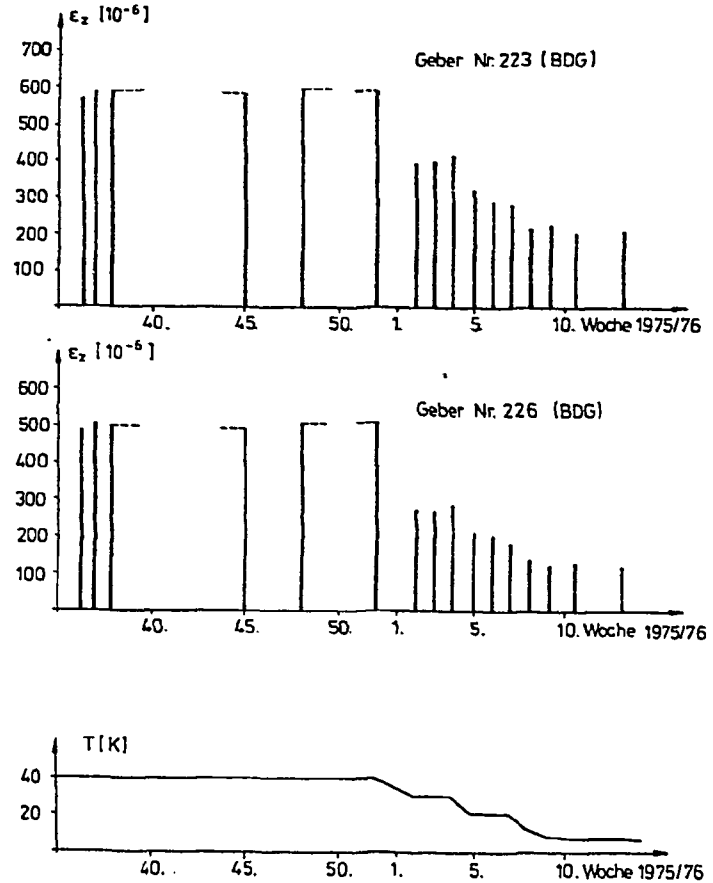


Fig. 7 Strains under 60 bar pressure, line XI

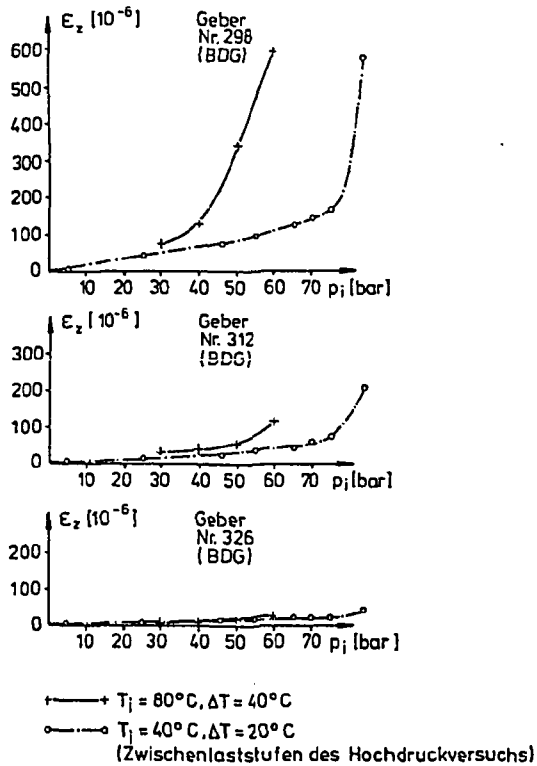


Fig. 8 Strains versus load, line XIII

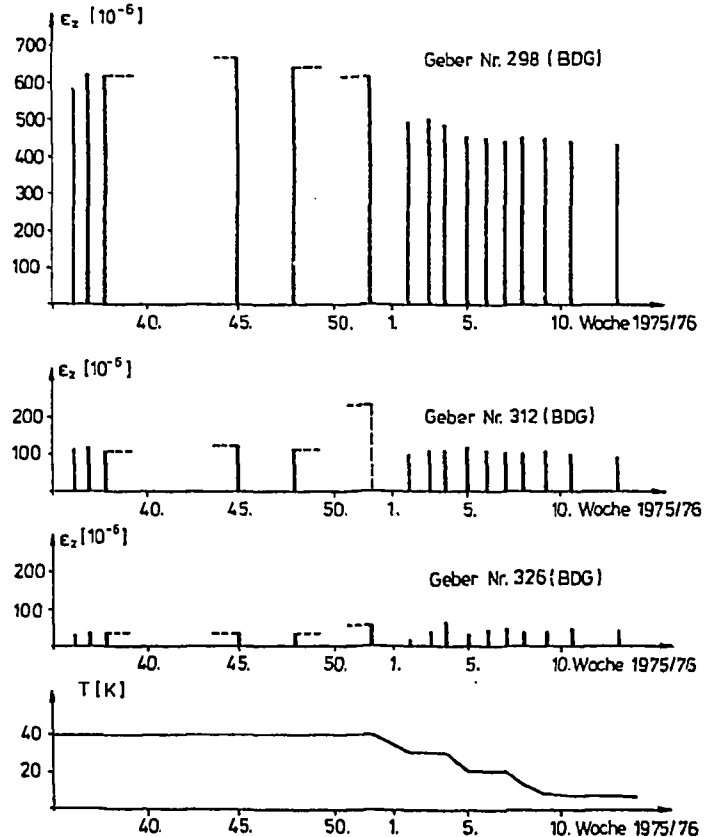


Fig. 9 Strains under 60 bar pressure, line XIII

Fig. 10  
Crack propagation at the surface

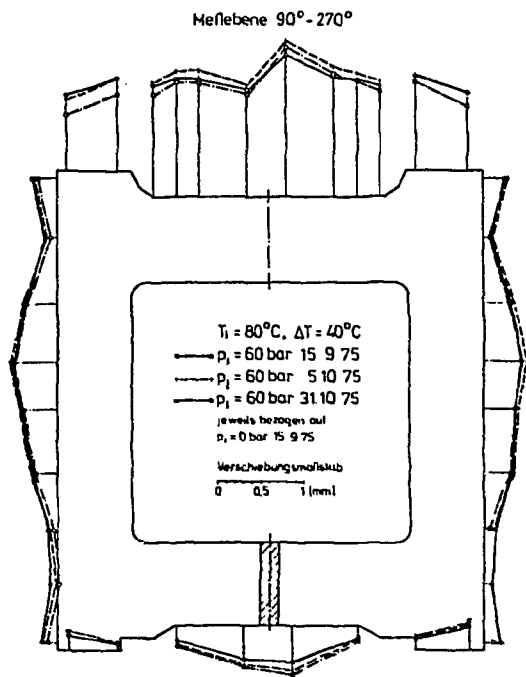
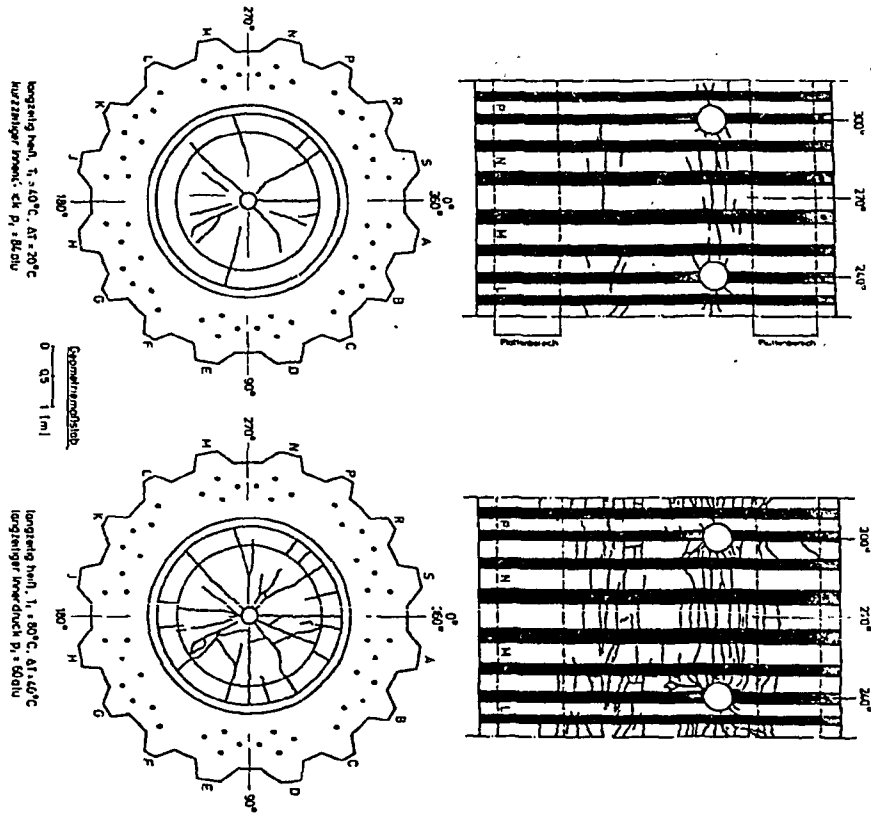


Fig. 11  
Displacements of surface  
under long-time pressure (phase 16)

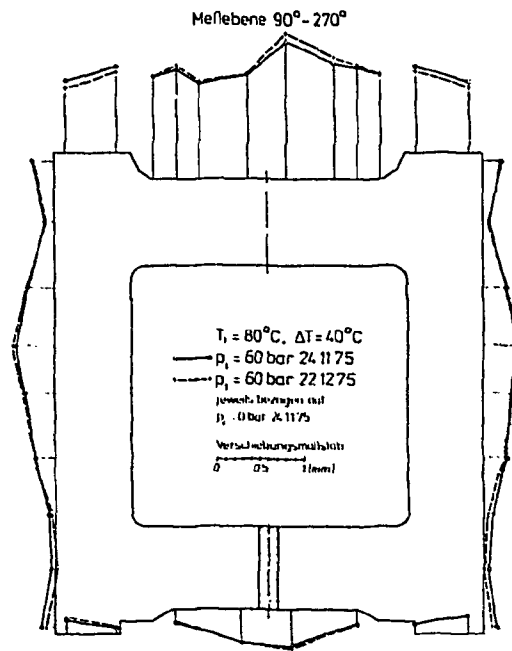


Fig. 12  
Displacements of surface  
under long-time pressure (phase 18)

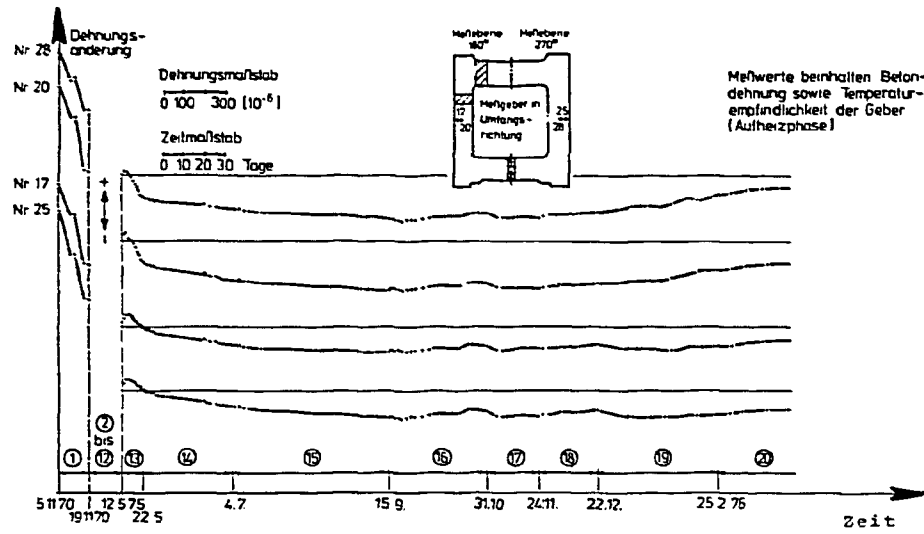


Fig. 13  
Creep behaviour (changes of tangential strains at equator)

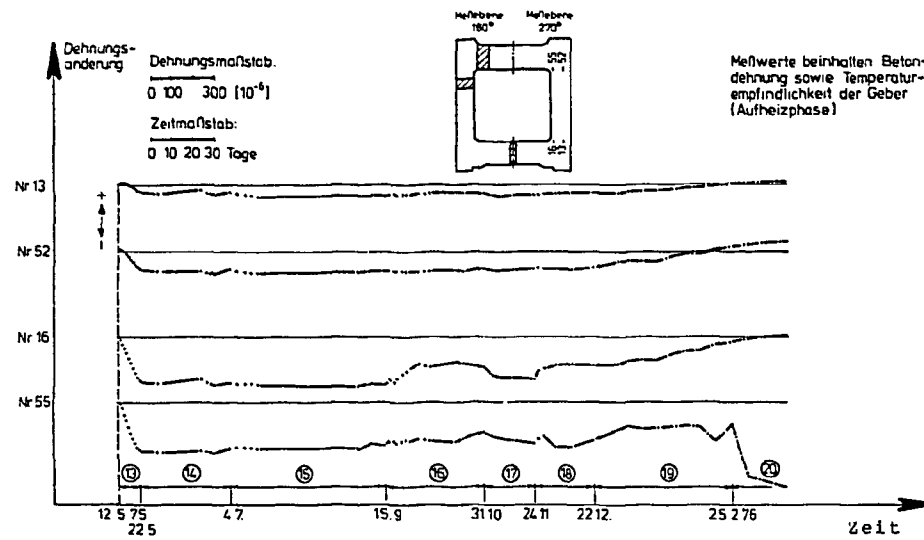


Fig. 14 Creep behaviour (changes of vertical strains in haunch regions)

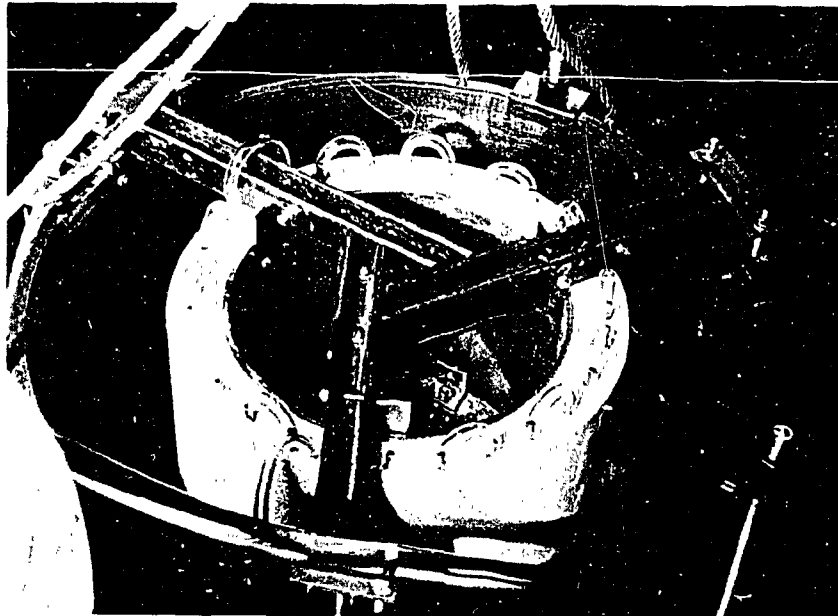


Fig. 15  
THTR resin model,  
air cooling system  
in inner mould

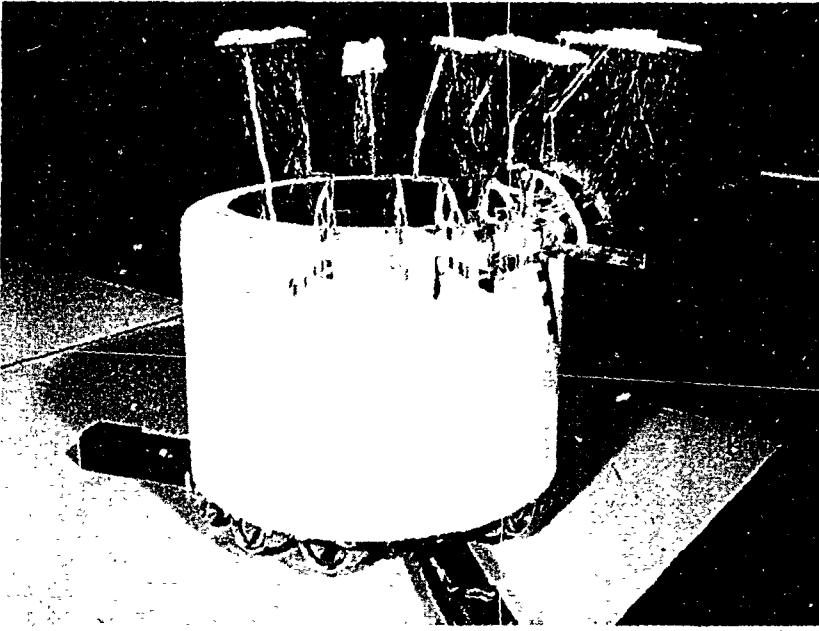


Fig. 16  
THTR resin model,  
inner mould with  
supports for embedded  
strain ganges

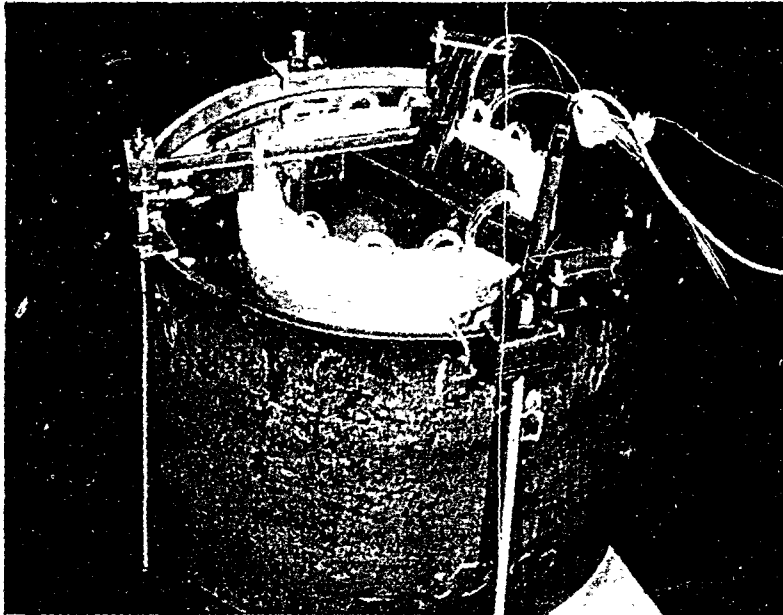


Fig. 18  
THTR resin model,  
mould ready  
for casting



Fig. 17  
Support for embedded  
strain ganges

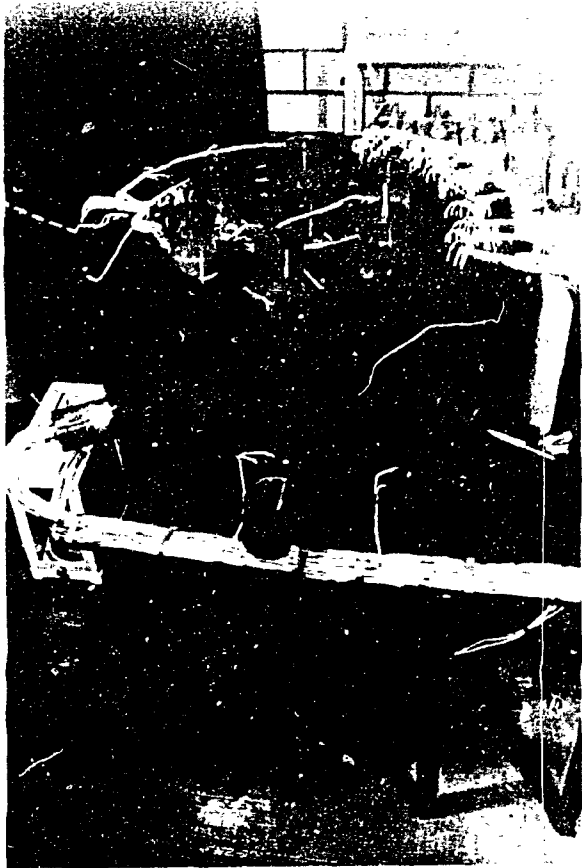


Fig. 19  
THTR resin model ready for testing

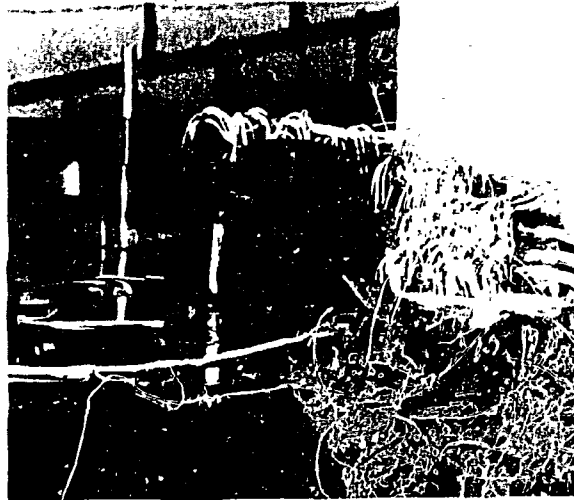


Fig. 20  
THTR resin model,  
detail of upper region

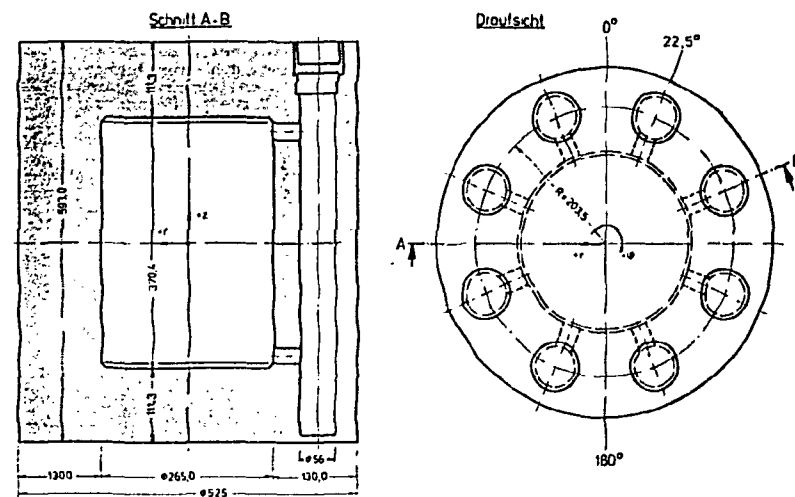


Fig. 21  
Hartlepool resin model, geometry

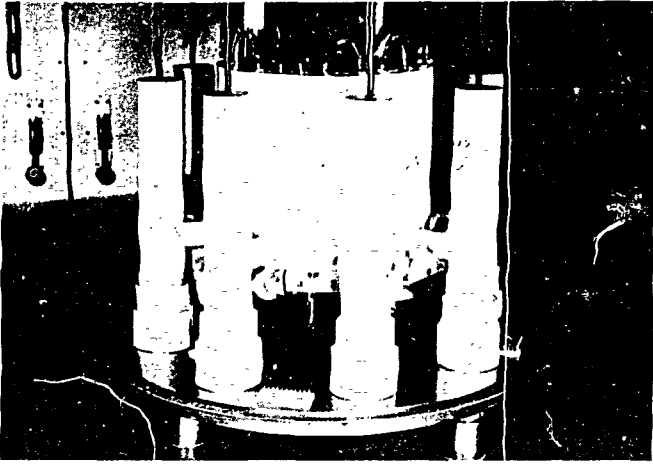


Fig. 22  
Hartlepool resin model, inner mould



Fig. 24  
Hartlepool resin model  
ready for testing

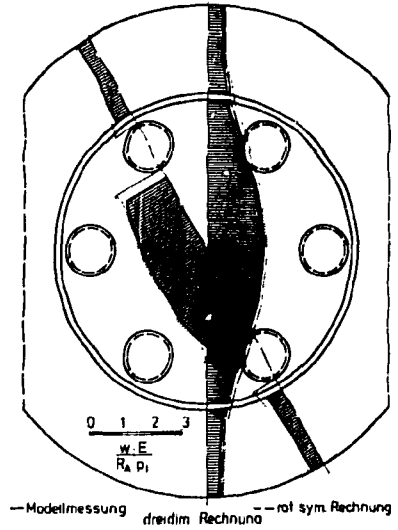


Fig. 25  
THTR resin model,  
vertical displacements  
of top slab

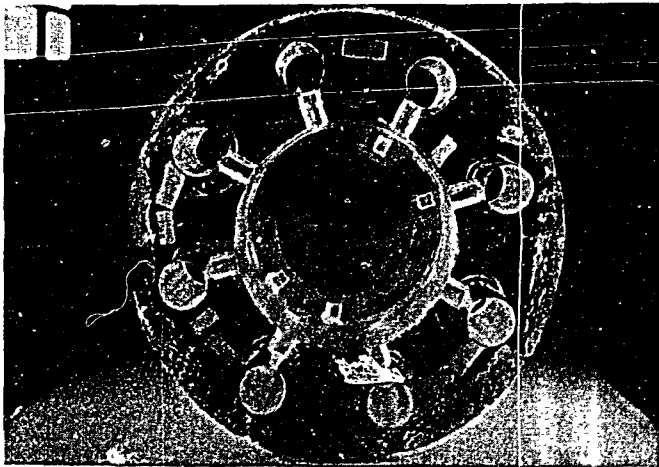


Fig. 23  
Hartlepool resin model, upper half after removing the mould

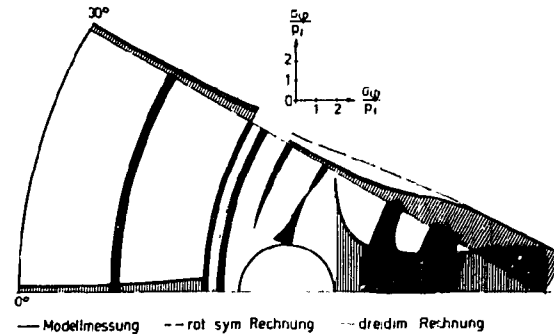


Fig. 26  
THTR resin model,  
circumferential stresses  
at top slab surface

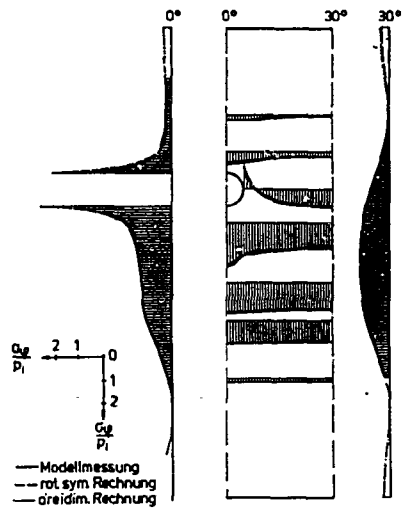
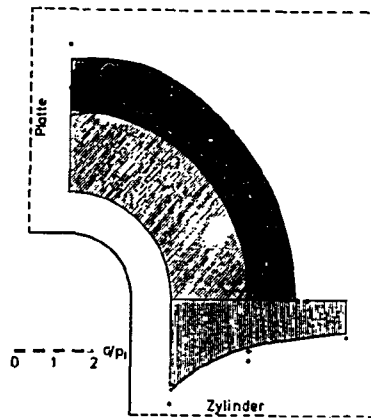


Fig. 27  
THTR resin model,  
circumferential stresses  
at surface of cylindrical wall



Messergebnisse: • Achse zwischen den Öffnungen  
• untere Modellhälfte

Fig. 28  
THTR resin model,  
stresses in haunch region

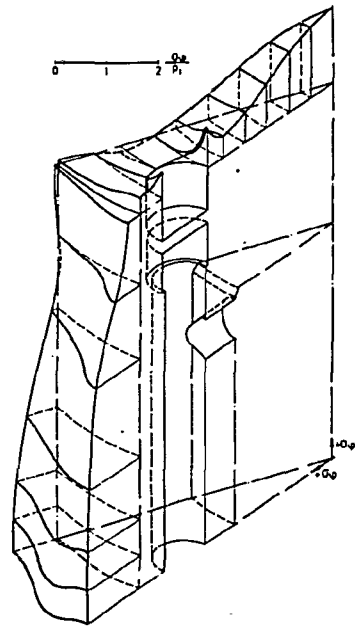


Fig. 29  
Hartlepool resin model,  
circumferential stresses  
at outer surface

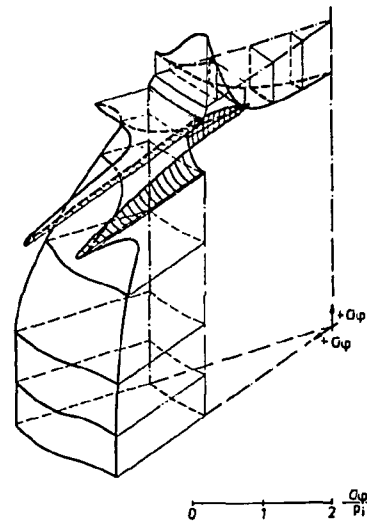


Fig. 30  
Hartlepool resin model,  
circumferential stresses at surface  
of core cavity

Fig. 32  
Hartlepool resin model,  
principal stresses  
in haunch region

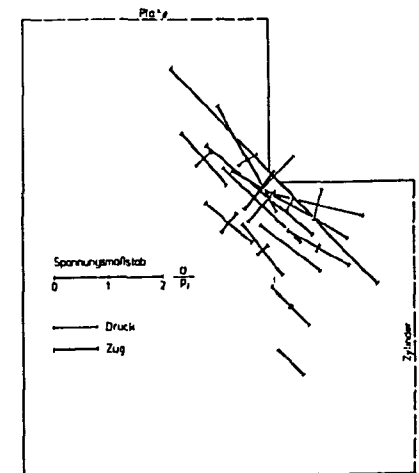


Fig. 31  
Hartlepool resin model,  
circumferential stresses  
in equator section

